Cellular Signalling 107 (2023) 110676

Contents lists available at ScienceDirect

Cellular Signalling

journal homepage: www.elsevier.com/locate/cellsig

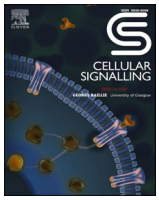

Asymmetric dimethylarginine positively modulates calcium-sensing receptor signalling to promote lipid accumulation

Laura Dowsett [a,b,*], Lucie Duluc [b], Erin Higgins [a], Fatmah Alghamdi [a], Walter Fast [c], Ian P. Salt [a,d], James Leiper [a,b]

[a] School of Cardiovascular and Metabolic Health, College of Medical, Veterinary and Life Sciences, University of Glasgow, Glasgow G12 8QQ, UK
[b] MRC London Institute of Medical Sciences, Imperial College London, London W12 0NN, UK
[c] Division of Chemical Biology and Medicinal Chemistry, University of Texas, Austin, TX 78712, USA
[d] School of Molecular Biosciences, College of Medical, Veterinary and Life Sciences, University of Glasgow, Glasgow G12 8QQ, UK

ARTICLE INFO

Keywords:
Asymmetric dimethylarginine
Calcium-sensing receptor
Obesity
Adipocytes
Hepatocytes
Adipocyte hypertrophy

ABSTRACT

Asymmetric dimethylarginine (ADMA) is generated through the irreversible methylation of arginine residues. It is an independent risk factor for cardiovascular disease, currently thought to be due to its ability to act as a competitive inhibitor of the nitric oxide (NO) synthase enzymes. Plasma ADMA concentrations increase with obesity and fall following weight loss; however, it is unknown whether they play an active role in adipose pathology. Here, we demonstrate that ADMA drives lipid accumulation through a newly identified NO-independent pathway via the amino-acid sensitive calcium-sensing receptor (CaSR). ADMA treatment of 3T3-L1 and HepG2 cells upregulates a suite of lipogenic genes with an associated increase in triglyceride content. Pharmacological activation of CaSR mimics ADMA while negative modulation of CaSR inhibits ADMA driven lipid accumulation. Further investigation using CaSR overexpressing HEK293 cells demonstrated that ADMA potentiates CaSR signalling via G_q intracellular Ca^{2+} mobilisation. This study identifies a signalling mechanism for ADMA as an endogenous ligand of the G protein-coupled receptor CaSR that potentially contributes to the impact of ADMA in cardiometabolic disease.

1. Introduction

Methylarginines are formed via the methylation of arginine residues by protein arginine methyltransferases (PRMT) [1]. The PRMT family consists of nine enzymes each encoded by a separate gene. These methylate histone proteins which act as key steps in transcriptional regulation, and a wider range of non-histone proteins involved in protein synthesis. All PRMT enzymes are capable of forming L-N^G monomethylated arginine (L-NMMA); while type I PRMTs, primarily PRMT1, form asymmetric dimethylarginine (ADMA), type II PRMTs, predominantly PRMT5, form symmetric dimethylarginine (SDMA). Unlike other post-translational modifications, arginine methylation is irreversible and therefore, proteolysis generates a constant flow of free methylarginines. These are initially released into the cytosol from where they may exit the cell to the circulation and ultimately be cleared by the kidney [2]. Previous studies, from our group and others, have demonstrated that asymmetrically methylated methylarginines (L-NMMA and ADMA) are competitive inhibitors of all three isoforms of nitric oxide synthase (NOS) [3–5]. In contrast, SDMA has no inhibitory action on NOS. As plasma ADMA concentrations are ~10-fold higher than that of L-NMMA it is thought ADMA is the most significant endogenously produced inhibitor of NO synthesis.

Relatively modest increases in ADMA in both humans and experimental models are associated with a profound disruption in cardiovascular homeostasis and have been linked to increased risk of hypertension, atherosclerosis and stroke [5–7]. Further, clinical studies have associated elevated circulating ADMA concentrations with obesity and the metabolic syndrome [8–14]. Although concentrations can vary widely between studies, dependent on the analytical methods used, on average an increase by 0.3 μM from ~0.58 μM to ~0.86 μM has been observed when assessed by mass spectrometry techniques. ADMA is also known to accumulate in the visceral adipose tissue of obese subjects [12,15] and circulating ADMA levels decrease following weight loss [10,14,16]. However, causal mechanisms between ADMA and adipose

* Corresponding author at: School of Cardiovascular and Metabolic Health, College of Medical, Veterinary and Life Sciences, University of Glasgow, Glasgow G12 8QQ, UK.
E-mail address: laura.dowsett@glasgow.ac.uk (L. Dowsett).

https://doi.org/10.1016/j.cellsig.2023.110676
Received 22 November 2022; Received in revised form 10 March 2023; Accepted 3 April 2023
Available online 5 April 2023

pathology have not been identified. Interestingly, NO levels are also increased in obesity and correlate with both BMI and adiposity [17] with increased expression of eNOS and iNOS found in the adipose tissue of obese individuals [18]. These observations might suggest additional roles of ADMA in adipose tissue that are independent of NOS. Utilising the 3T3-L1 cell line, we set out to test the hypothesis that ADMA regulates adipocyte function and physiology via a NO-independent mechanism. Upon establishing that NO-independent pathways exist in adipocytes we then went on to test the hypothesis that ADMA may act via the amino-acid sensitive calcium-sensing receptor in vitro.

2. Methods

2.1. Contact for reagents and resource sharing

Further information and requests for resources and reagents should be directed to the Lead Contact, Laura Dowsett (laura.dowsett@glasgow.ac.uk).

2.2. Cell lines

The murine pre-adipocyte 3T3-L1 cell line was purchased from American Type Culture Collection (ATCC CL-173) and sub-cultured in low glucose (1 g/l) Dulbecco's modified Eagle's Medium (DMEM) supplemented with 10% new-born calf serum, 1× penicillin-streptomycin and 2 mM L-glutamine at 37 °C in a humidified atmosphere with 5% CO_2. To stimulate differentiation to mature adipocytes, 2-day post-confluent cells were exposed to high glucose (4.5 g/l) DMEM supplemented with 10% foetal bovine serum (FBS) and containing 10 μg/ml insulin (Sigma-Aldrich, I9278), 1 μM dexamethasone (Sigma-Aldrich, D1756) and 0.5 mM isobutyl-methylxanthine (Sigma-Aldrich, I5879). At day 2 induction media was replaced with supplemented DMEM containing 10 μg/ml insulin only. At day 4 cells were then cultured a further 4 days in high glucose DMEM. Adipocytes were considered mature at 10 days post induction.

The human hepatoma cell line HepG2 was purchased from American type Culture Collection (ATCC HB-8065) Cells were maintained at 37 °C in a humidified atmosphere with 5% CO_2 in DMEM supplemented with 10% FBS, 2 mM glutamine and 1% penicillin-streptomycin.

Inducible CaSR overexpressing cells were generated using the Flp-In T-REx HEK-293 cell line using the protocol developed by Ward et al. [19]. The N-terminal Myc-tagged human CaSR gene was inserted into the pcDNA5-FRT-TO plasmid by Genscript. The pcDNA5-FRT-TO and the pOG44 plasmids were transfected using Lipofectamine 2000 (ThermoFisher). Positive cells were selected using hygromycin B. CaSR expression was induced by 0.5 μg/ml doxycycline treatment for 24 h.

2.3. 3T3-L1 treatments

Cell size experiments in mature 3T3-L1 adipocytes were performed for 72 h with either ADMA (1, 3 and 10 μM, Calbiochem, 311,203), SDMA (10 μM, Calbiochem, 311,204), 1,3-PB-ITU, dihydrobromide (20 μM, Sigma-Aldrich), and L-Nitroarginine methyl ester (L-NAME, 1 mM, Sigma-Aldrich, N5751) treatment. Experiments to assess mRNA and protein levels were performed over 48 h including those to explore mTOR inhibition by rapamycin (10 nM, Sigma-Aldrich, R8781), and effects by NO donors S-Nitroso-*N*-acetyl-DL-penicillamine (SNAP, 100 μM Calbiochem, 487,910) and 8-Bromo-Guanosine 3′,5′-cyclic Monophosphate (8-bromo-cGMP, 100 μM Calbiochem 203,820). The role of CaSR was assessed by the positive allosteric modulator Cinacalcet hydrochloride (100 nM, Tocris, 6170/10) and negative allosteric modulators NPS-2143 hydrochloride (10 μM, Tocris, 3626/10), Calhex 231 hydrochloride (1 μM, Tocris, 4387/10) over 48 h.

2.4. HepG2 treatments

HepG2 cell treatments were performed as above but over an 18-h time course for studies exploring mRNA expression.

2.5. Triglycerides and cholesterol quantification

Triglyceride content was measured using the Triglyceride Quantification Assay kit from Abcam (ab65336) and total cholesterol content was assessed with Amplex Red Cholesterol Assay Kit from Invitrogen (A12216) according to manufacturer's instructions.

2.6. SREBP -1 transcription factor assay

Fully differentiated 3T3-L1 cells were treated for 6 h with 10 μM ADMA. Nuclear extracts were made using the nuclear extraction kit from Abcam (ab113474). Nuclear SREBP-1 was detected using the SREBP-1 transcription factor assay kit from Abcam (ab133125).

2.7. Insulin sensitivity

Glucose uptake was measured by the uptake of 2-[^{3}H]-deoxy-D-glucose as described previously [20]. Briefly, 3T3-L1 adipocytes were stimulated with 10 μM ADMA for 48 h, the medium removed and replaced with Krebs-Ringer-phosphate (KRP (128 mM NaCl, 4.7 mM KCl, 5 mM NaH_2PO_4 (pH 7.4), 1.2 mM $MgSO_4$, 2.5 mM $CaCl_2$, 1% (*w/v*) BSA, 3 mM glucose)) buffer containing 10 μM ADMA. After incubation for 1 h at 37 °C, cells were incubated in insulin (0–100 nM) for 12 min and glucose transport was initiated by adding [^{3}H]-2-deoxyglucose (50 μM, 2 μCi/ml). Cells were incubated for 3 min, after which cells were rapidly washed in ice-cold PBS, air-dried, and then solubilized in 1% (*v/v*) Triton X-100. The radioactivity associated with the cells was determined by liquid scintillation spectrophotometry. Non-specific cell-associated radioactivity was determined in parallel incubations performed in the presence of 10 μM cytochalasin B.

2.8. RNA isolation and Rt-qPCR analysis

RNA was extracted and isolated using Qiagen's Universal RNeasy Kit. cDNA was synthesised from total RNA with iScript cDNA Synthesis kit (Bio-rad). qPCR's were run on the 7900 Fast Real-time PCR system (Applied Biosciences) using SYBR green Supermix (Bio-rad). Fold changes in mRNA expression were calculated using the ΔΔCt method and normalised to 18S gene expression. Primer sequences were as follows: 18S forward - GCTCAGCGTGTGCCTACC, 18S reverse-GGCCTCACTAAACCATCCAA; murine mTOR forward- TTCAATCCATAGCCCCGTCT, murine mTOR reverse - CAAAGAGCTGCATCACTCGT; human mTOR forward - GGCCGACTCAGTAGCAT, human mTOR reverse - CGGGCACTCTGCTCTTT; murine ACC forward – ATGGGCGGAATGGTCTCTT, murine ACC reverse - TGGGGACCTTGCTTTCATC; murine Hmgcr forward – CCAAACCCCGTAACCCAAAG, murine Hmgcr reverse – GATAAAACTGCCAGAGAGAAACACT; human Hmgcr forward – CTGCCAATGCTGCCATAAGT, human Hmgcr reverse – AGATAGGAACGGTGGGTGGT; human Ldlr forward – GACGTGGCGTGAACATCTG, human Ldlr reverse – CTGGCAGGCAATGCTTTGG.

2.9. Western blotting

Following protein electrophoresis and protein transfer, membranes were probed with primary antibodies from the following sources: mTOR antibody (Cell Signalling, #2972) and CaSR (Abcam, ab137408)). Loading controls were pan-actin (Cell Signalling #8456), and vinculin (Invitrogen #700062). Primary antibodies were used at 1:1000 and secondary antibodies at 1:5000 dilution. The relative intensity of the immune-reactive bands was determined by densitometry using Li-COR Image Studio Software. The results were normalised to the loading

protein and expressed as fold change over control.

2.10. Immunohistochemistry

Cells were plated on coverslips, cultured and then fixed for 10 min with 4% formaldehyde solution in PBS at room temperature, washed in PBS for 5 min and incubated in 3% BSA, 0.1% Triton-X100 blocking buffer in PBS for 1 h at room temperature. Cells were incubated with rabbit anti-CaSR antibody (Abcam #137408) at 1:200 dilution overnight in 3% BSA at 4 °C before washing with 0.1% Triton -X100 in PBS. Secondary antibodies (Alexafluor 488, ThermoFisher) were incubated for 2 h at room temperature before washing and mounting with Prolong Diamond Antifade with DAPI (ThemoFisher).

2.11. Bodipy

Cells were cultured on coverslips, stimulated with various treatments and then fixed for 10 min with 4% formaldehyde solution in PBS, washed in PBS for 5 min then incubated in PBS containing 1 μg/ml Bodipy (ThermoFisher, D3921) for 15 min. Coverslips were mounted in Prolong Diamond with DAPI mounting media. Pictures were taken under a confocal laser scanning fluorescence microscope (Leica TCS SP5). Cell size was determined using the NIH ImageJ Software package. Three images were captured per coverslip. Starting in the bottom right of each image 30 cells (or all cells if <30) were analysed. Average lipid area was assessed by thresholding of total BODIPY area and divided by the number of BODIPY positive cells. Data was plotted as an average of 3 images per experiment.

2.12. Intracellular Ca^{2+} imaging

HEK293-CaSR cells were incubated at 37 °C with 1 μM Cal520 (Abcam, ab171868) in Optimem Reduced Serum I medium (HEPES, 2.4 g/l Sodium Bicarbonate, L-glutamine) containing relevant treatments for 1 h before imaging. Cells were then washed and incubated in Ca^{2+} – free HEPES buffer (130 mM NaCl, 5 mM KCl, 1 mM $MgCl_2$, 20 mM HEPES, 10 mM Glucose, pH 7.4) containing relevant treatments. Gd^{3+} was used as a CaSR agonist (0.01 mM–5 mM), NPS-2143 was used as a CaSR negative allosteric modulator (10 μM). Changes in cytosolic Ca^{2+} were imaged using a Zeiss ZenPro inverted microscope; and FITC fluorescence determined using the physiology definition programme as part of the Zen Software (Zeiss Microscopy GmbH, Germany). Data are represented as the change in fluorescence (FΔ) over the fluorescence at baseline (F0) normalised to the maximum control response to each experiment.

2.13. Quantification and statistical analysis

Statistical analyse were performed using GraphPad Prism 9 Software. Comparisons were carried out with unpaired two-tailed Student's *t*-test, One-way ANOVA with Bonferroni multiple comparison tests or Two-way ANOVA with Sidak's multiple comparison test as appropriate. Dose response curves were assessed by non-linear regression. Statistical significance was accepted for $P < 0.05$. Data are expressed as mean ± SEM. All in vitro experiments are a mean of at least three independent experiments, numbers for each experiment are confirmed in the figure legends.

3. Results

3.1. ADMA induces lipid accumulation in 3T3-L1 cells through a NO-independent pathway

To evaluate the consequences of ADMA exposure on adipocyte function we utilised the mouse 3T3-L1 cell line as a model for mature adipocytes. 3T3-L1 fibroblasts were differentiated to lipid laden cells via the addition of insulin, dexamethasone and isobutyl-methylxanthine. 3T3-L1 cells were considered fully differentiated 10 days post-induction, at which point they were treated with ADMA for an additional 72 h. ADMA concentrations were chosen to reflect those occurring in disease. 3T3-L1 cells treated with 1, 3, and 10 μM ADMA all showed significant cellular hypertrophy compared to those cultured in control media (Fig. 1a and b); whereas SDMA (10 μM) had no effect. Given the currently understood mechanism of action of ADMA as a competitive inhibitor of NOS, we assessed the effect of two structurally distinct synthetic NOS inhibitors N(g)- nitro-L-arginine methyl ester (L-NAME, 1 mM) and 1,3-PBI-TU dihydrobromide (20 μM) at concentrations which maximally block NO production. Interestingly, these did not cause adipocyte hypertrophy suggesting that the effect of ADMA on cell size may be independent of NOS inhibition.

In order to identify the potential mechanism through which ADMA is acting, we first established whether cellular hypertrophy was due to increased lipid content. Adipocytes treated with 3 μM and 10 μM ADMA had increased lipid area per cell as assessed using BODIPY staining (Fig. 1c). Correspondingly, cells treated with 3 μM ADMA had increased intracellular cholesterol and triglyceride content (Fig. 1d). Taken together these data suggest that a NO independent mechanism specific to ADMA drives adipocytes hypertrophy in 3T3-L1 cells.

3.2. ADMA treatment upregulates a suite of lipogenic genes in 3T3-L1 cells

To investigate the effect of ADMA on de-novo lipid synthesis we assessed the involvement of sterol regulatory element-binding protein-1 (SREBP-1) signalling. ADMA (10 μM) treatment of 3T3-L1 cells for 6 h increased SREBP-1 nuclear accumulation (Fig. 2a). We also found that exposure to ADMA increased the mRNA expression of SREBP-1 downstream target genes acetyl-CoA carboxylase (ACC), fatty acid synthase (FASN) and HMG-CoA reductase (HMGCR) (Fig. 2b). As mTOR (mammalian target of rapamycin) is important for SREBP-1 cleavage [21] we measured its mRNA and protein expression. We found that ADMA induced the expression of mTOR at both the mRNA (Fig. 2c) and protein levels (Fig. 2d and e); an effect that was not reproduced by SDMA or NOS inhibition. Rapamycin treatment over 48 h was used to confirm the involvement of mTOR. Rapamycin (10 nM) blocked ADMA induced cellular hypertrophy and the induction of ACC expression (Fig. 2f and g) suggesting ADMA can signal via the mTOR pathway. Inhibition of NOS had no effect on mTOR expression; however, we wanted to confirm that stimulation of NO signalling also had no effect on these pathways. All 3T3-L1 studies were completed in DMEM medium which contains 400 μM L-arginine as standard, however given the 'arginine paradox' [22] it is well known that additional L-arginine can further stimulate NO production. However, the addition of a further 100 μM L-arginine had no effect on the expression of either ACC or FASN (Fig. 2h). Equally, the NO donor S-nitroso-N-Acetyl-D, L-penicillamine (SNAP) as well as the stable cGMP analogue 8-bromo-cGMP had no effect on mTOR expression (Fig. 2i) suggesting NO does not regulate this pathway. ADMA had no effect on glucose uptake suggesting it is not altering the insulin signalling pathway in 3T3-L1 cells (Fig. 2j).

3.3. ADMA induces lipogenesis in HepG2 cells

As the liver is a significant site for ectopic fat deposition, we assessed whether ADMA could induce lipid accumulation in the human hepatocyte-derived HepG2 cell line. Here, ADMA increased the lipid content of HepG2 cells, as evidenced by increased BODIPY staining (Fig. 3a). Which was confirmed by an ADMA induced increase in HepG2 triglyceride content (Fig. 3b). As with 3T3-L1 cells SDMA and NOS inhibitors had no effect on lipid accumulation. ADMA again increased the expression of ACC but in HepG2 cells also decreased the expression of the low-density lipoprotein receptor (Ldlr) (Fig. 3c). We also found ADMA upregulated mTOR expression in HepG2s (Fig. 3d). Having had no effect on lipid accumulation we confirmed that SDMA treatment of

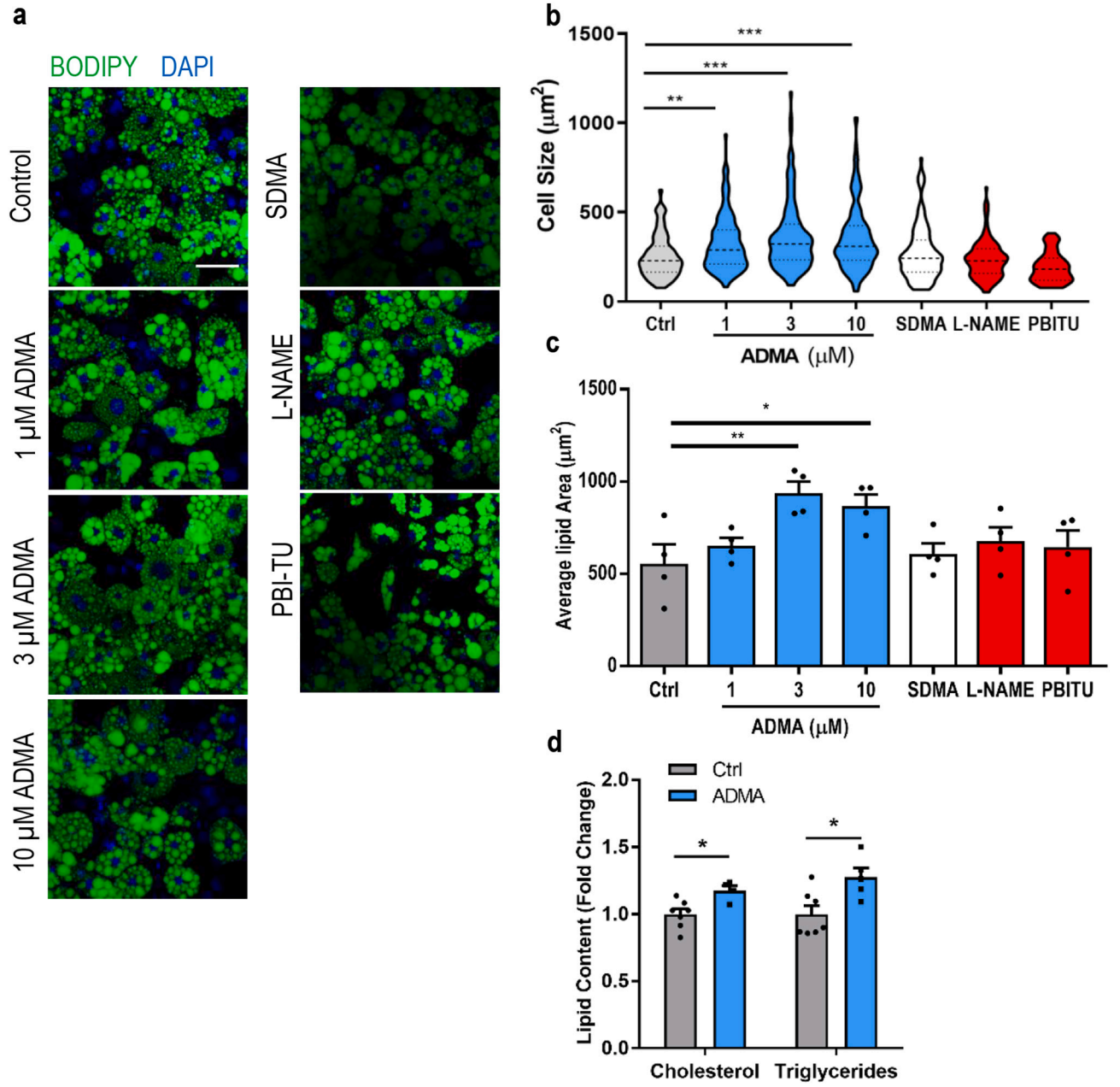

Fig. 1. ADMA promotes lipid accumulation through a NO-independent mechanism in 3T3-L1 cells.
(a - c) 3T3-L1 cells were treated for 72 h with ADMA, 10 μM SDMA, 1 mM L-NAME and 20 μM PBI-TU and were **(a)** stained with BODIPY and DAPI, (representative images from 3 independent experiments, scale bar 50 μm). Cells were measured to establish **(b)** cell area and **(c)** the average lipid area per cell (155 cells from 4 independent experiments). **(d)** 3T3-L1 cholesterol and triglyceride content following 3 μM ADMA treatment for 72 h ($N = 7$). One-way ANOVA with Bonferroni *post-hoc* test was used in **b, c**; and two-tailed student's *t*-test in **d**. * $P < 0.05$, ** $P < 0.01$, *** $P < 0.001$. Data are presented as mean ± S.E.M.

HepG2 cells had no effect on mRNA expression of ACC (Fig. 3e). Like 3T3-L1 cells HepG2 are cultured in standard DMEM media with 400 μM L-arginine present, and again the addition of a further 100 μM L-arginine had no effect on ACC expression suggesting NO is not regulating this pathway in HepG2 cells. HepG2 cells treated with rapamycin could not replicate the ADMA driven upregulation of ACC (Fig. 3f). These data indicate that the effects of ADMA are seen in two of the most highly lipogenic cell types and in both mouse and human cells through the upregulation of lipogenic pathways.

3.4. ADMA induced lipogenesis via CaSR activation in 3T3-L1 cells

In comparison to the concentration of ADMA required for significant NOS inhibition in cell culture systems (100 μM) the concentration of ADMA we have identified as capable of driving adipocyte hypertrophy is low (1–10 μM). At this concentration ADMA entry into cells via the cationic amino acid transporter is likely to be limited due to competition from the high concentration of cationic amino acids, including L-arginine, in the culture media [23]. Therefore, we hypothesised that ADMA may act via an extracellular receptor. The calcium-sensing receptor (CaSR) is a member of the class C family of amino-acid sensitive GPCRs. CaSR is expressed in both adipocytes and hepatocytes [24] and has been linked to adipose dysfunction and fat accumulation [25,26]. Although the primary ligand for CaSR is calcium itself, it has been shown that CaSR has a secondary binding pocket where amino acids such as phenylalanine and tryptophan can bind and act as positive allosteric

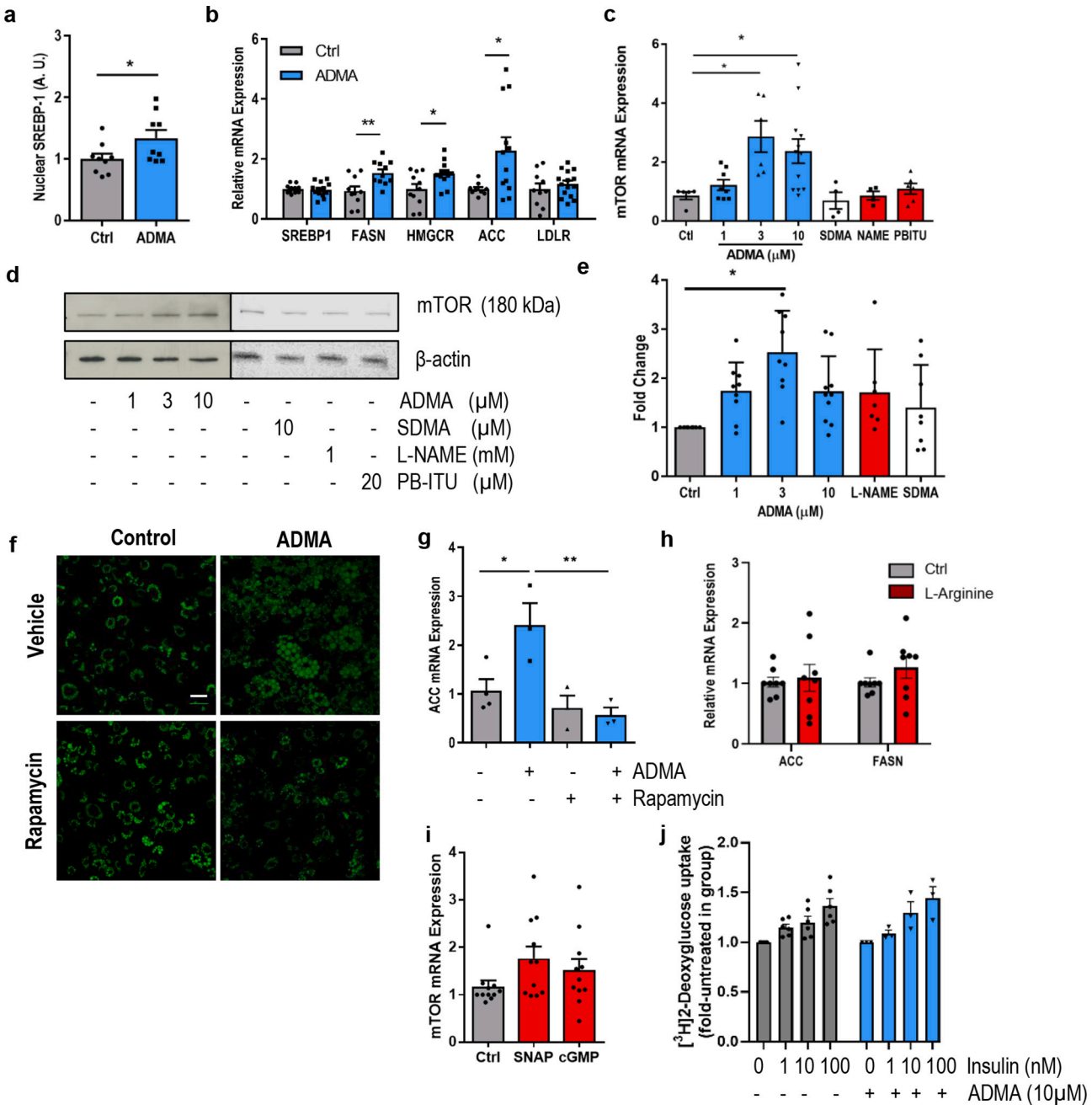

Fig. 2. ADMA upregulates lipogenic pathways in 3T3-L1 cells.
(a) Nuclear SREBP-1 levels in 3T3-L1 adipocytes following 6 h stimulation with 10 μM ADMA ($N = 9$, A.U. Arbitrary units). **(b)** qPCR analysis of SREBP target genes after stimulation of 3T3-L1 cells with 3 μM ADMA for 12 h, values are fold change normalised against 18S housekeeper gene ($N = 12$). SREBP1: Sterol regulatory element-binding protein 1, FASN: Fatty acid synthase, HMGCR: HMG—CoA reductase, ACC: Acetyl-CoA Carboxylase, LDLR: Low density lipoprotein receptor. **(c)** qPCR analysis of mTOR mRNA expression ($N = 5$) and **(d and e)** western blot analysis of mTOR levels following 48 h incubation of 3 T3-L1 cells with ADMA, 10 μM SDMA, 1 mM L-NAME and 20 μM PBI-TU (N = 7). Actin was used as a loading control, representative immunoblots. **(f)** BODIPY staining of 3T3-L1 cells incubated with 10 μM ADMA with or without rapamycin (10 nM) for 72 h, representative images, scale bar 50 μm. **(g)** qPCR analysis of Acetyl-Co A Carboxylase (ACC) expression after incubation of 3T3-L1 cells with ADMA (48 h, 10 μM) in the presence or absence of 10 nM rapamycin ($N = 3$). **(h)** qPCR analysis of Acetyl-CoA Carboxylase (ACC) and Fatty acid synthase (FASN) expression in 3T3 – L1 cells treated with an additional 100 μM L-arginine for 48 h. **(i)** qPCR of mTOR expression in 3T3-L1 adipocytes after 48 h in the presence of 100 μM SNAP or 100 μM 8-bromo-cGMP ($N = 10$). **(j)** [^{3}H]2- deoxyglucose uptake following 10 μM ADMA treatment and insulin (0-100 nM) stimulation. All qPCR data are expressed as fold change normalised to 18S expression. One-way ANOVA with Bonferroni *post-hoc* test was used in **c, e, and h**; two-tailed students t-test in **a and b** and two-way ANOVA in **g and i** with Sidak's *post-hoc* test. Data are presented as mean ± S.E.M. * $P < 0.05$, ** $P < 0.01$, *** $P < 0.001$.

modulators (PAMs) [27,28]. Therefore, we hypothesised that ADMA may be able to modulate fat accumulation via the CaSR.

We confirmed CaSR expression within our 3T3-L1 and HepG2 cultures (Supplementary Fig. 1) and that CaSR expression was unaffected by 3T3-L1 differentiation (Fig. 4a). To confirm that in our hands CaSR activation causes hypertrophy and lipid accumulation in 3T3-L1 cells we treated them with the PAM cinacalcet (100 nM). Cinacalcet treatment achieved similar levels of adipocyte hypertrophy and lipid accumulation as 10 μM ADMA (Fig. 4b-d). We then investigated whether negative regulation of CaSR blocked the lipogenic effects of ADMA on 3T3-L1

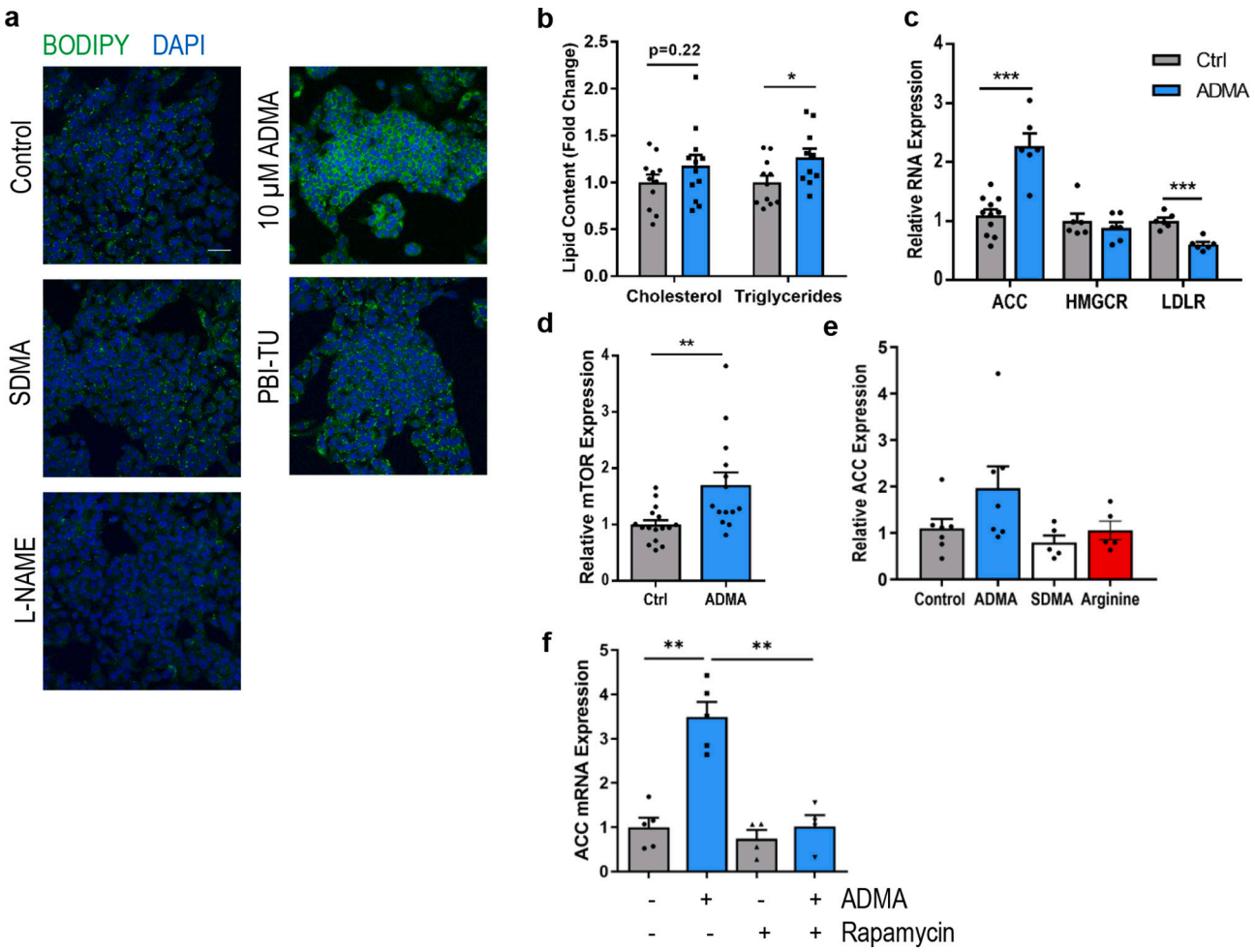

Fig. 3. ADMA induces lipid accumulation in the HepG2 cell line.
(a) HepG2 cells treated for 48 h with 10 μM ADMA, 10 μM SDMA, 1 mM L-NAME and 20 μM PBI-TU and were stained with BODIPY for lipid accumulation (representative images). **(b)** HepG2 cholesterol and triglyceride content following 10 μM ADMA treatment for 48 h ($N = 11$). **(c)** qPCR analysis of lipogenesis gene mRNA expression in HepG2 cells incubated for 18 h with 10 μM ADMA, normalised against 18S expression ($N = 6$). ACC: Acetyl-CoA Carboxylase, HMGCR: HMG-CoA reductase, LDLR: Low density lipoprotein receptor. **(d)** qPCR analysis of mTOR expression in HepG2 cells after incubated for 18 h in 10 μM ADMA ($N = 12$). **(e)** qPCR analysis of ACC expression in HepG2 cells incubated with 10 μM SDMA or an additional 100 μM L-arginine for 18 h ($N = 6$). **(f)** qPCR analysis of ACC expression in HepG2 cells incubated for 18 h in 10 μM ADMA in the presence or absence of rapamycin (10 nM). Two-way ANOVA followed by Sidak's *post-hoc* was used in **e**; and two-tailed student's t-test in **b, c** and **d**. * $P < 0.05$, ** $P < 0.01$, *** $P < 0.001$. Data are presented as mean ± S.E.M.

cells. CaSR NAMs, Calhex-231 (10 μM) and NPS-2143 (10 μM), inhibited the lipogenic effect of ADMA on both adipocyte cell size and lipid area. Interestingly, NPS-2143 alone but not Calhex-231 caused an increase in 3T3-L1 cell size (Fig. 4e-g); but both compounds antagonised the effect of ADMA. Next, we investigated whether NPS-2143 treatment might inhibit ADMA driven upregulation of lipogenesis genes. Given that CaSR has previously been reported to upregulate PPARγ we included it in this analysis [29]. We found that ADMA too increases the expression of PPARγ and that this as well as the upregulation of FASN can be blocked by NPS-2143 (Fig. 4h and i). These data suggest that CaSR is a potential mechanism through which ADMA is regulating lipogenesis in 3T3-L1 cells.

3.5. ADMA increases CaSR sensitivity

CaSR is a promiscuous GPCR signalling through $G_{q\ \_}$ resulting in increased cytosolic Ca^{2+} mobilisation, $G_{i/o}$ inhibiting cAMP signalling and finally $G_{12/13}$ Rho signalling [30]. To determine if ADMA directly modifies CaSR activity we developed a HEK293-CaSR cell line using the Flp-In T-REx transfection system [19] which overexpresses CaSR following doxycycline treatment (Fig. 5a and b). For further experiments we choose to use 0.5 μg/ml doxycycline treatment as this seemed to induce maximal CaSR expression with no further effect at higher concentrations. To assess whether ADMA affects intracellular Ca^{2+} mobilisation we incubated cells in a Ca^{2+}-free HEPES buffer and used the highly potent CaSR agonist Gd^{3+} to increase $[Ca^{2+}]_i$ in a dose-dependent manner. Gd^{3+} and Cinacalcet did not stimulate intracellular Ca^{2+} mobilisation in vector only cells or HEK-CaSR cells untreated with doxycycline (data not shown). Alone Gd^{3+} caused a dose-depending increase in $[Ca^{2+}]_i$ (Fig. 5c). Pre-treatment with 10 μM ADMA increased CaSR sensitivity to Gd^{3+} (Fig. 5c and d) shifting the dose-response curve to the left (Control EC_{50}–0.2 mM, ADMA EC_{50}–0.06 mM) and to a similar degree as previously reported for other amino acids [31]. Pre-treatment with NPS-2143 completely inhibited the effect of ADMA on intracellular Ca^{2+} (Fig. 5e). As discussed in the introduction, L-arginine competes with ADMA for binding at the active site of the NOS enzymes, we investigated whether the same is true for the CaSR binding site. Figs. 5c-e had been performed in the absence of L-arginine therefore we increased L-arginine concentrations to physiological (80 μM) or supra-physiological (1 mM) levels, but neither influenced CaSR signalling, neither basally nor in the presence of ADMA (Fig. 5f). Thereby, suggesting that arginine does not a compete with ADMA at the CaSR

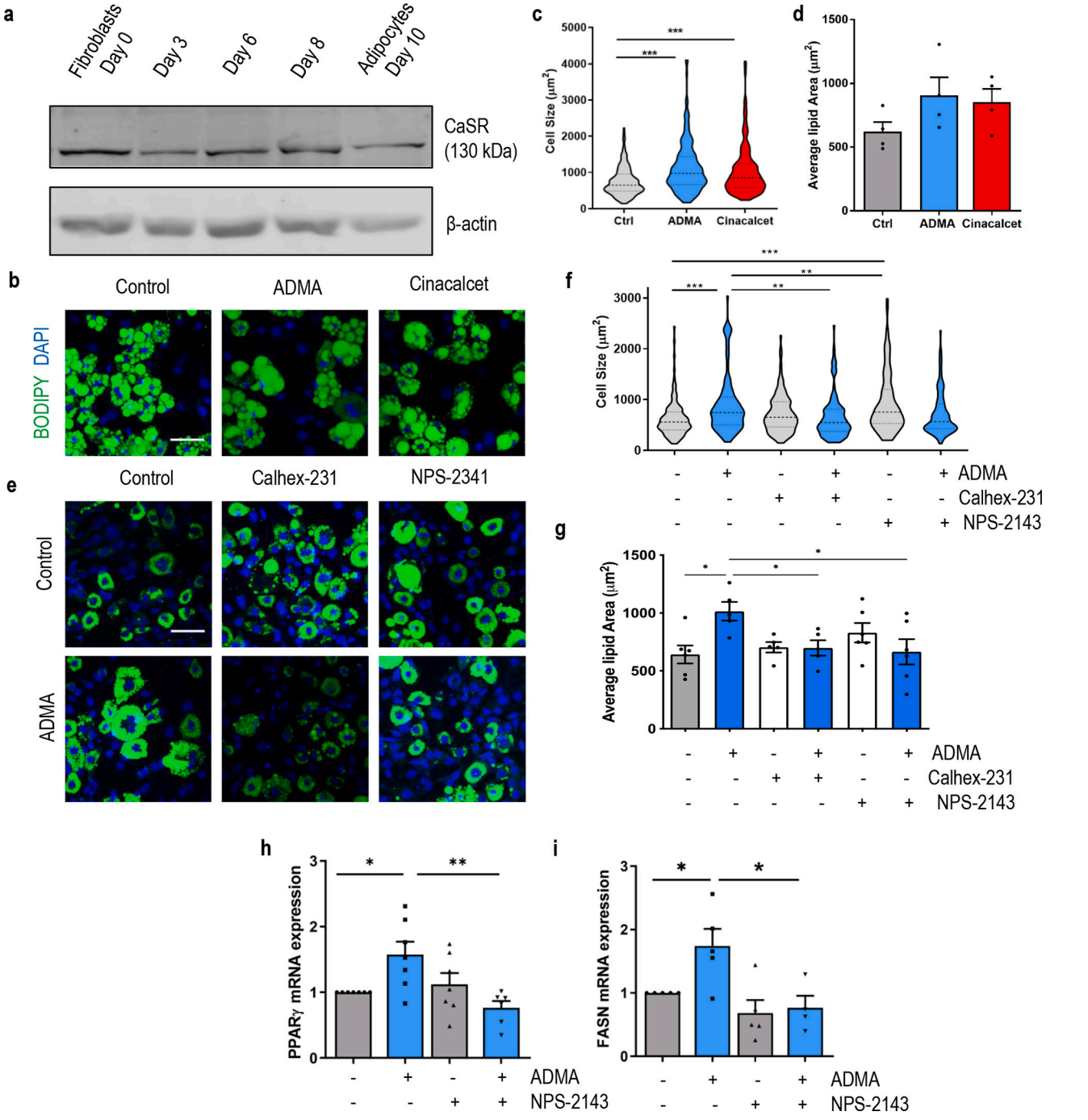

Fig. 4. ADMA driven lipid accumulation is mimicked by CaSR PAMs and blocked by CaSR NAMs in 3T3-L1 cells.
(a) Western blot analysis confirms CaSR expression is unaffected by 3T3-L1 differentiation. **(b-d)** 3T3-L1 cells incubated for 72 h with 10 μM ADMA or 100 nM Cinacalcet were **(b)** stained with BODIPY and DAPI. Data are representative images from 4 independent experiments, scale bar 100 μm and measured for **(c)** cell size and **(d)** average lipid area ($N = 160$ cells from 4 independent experiments).**(e-g)** 3T3-L1 incubated for 72 h with 10 μM ADMA in the presence of 10 μM Calhex-231 or NPS-2413 were **(e)** stained with BODIPY and DAPI, representative images from 3 independent experiments, scale bar corresponds to 100 μm and measured for **(f)** cell size ($N = 130$ cells from 3 independent experiments) and **(g)** average lipid area ($N = 5$). **(h and i)** qPCR analysis in 3 T3-L1 cells of **(h)** PPARγ and **(i)** FASN following 48 h treatment with 10 μM ADMA ±1 μM NPS-2143. One-way ANOVA with Bonferroni *post-hoc* test in **c,d, f** and **g;** Two-way ANOVA with Sidak's *post-hoc* test was used in **h**, and **i**. *P < 0.05, **P < 0.01, ***P < 0.001. Data are presented as mean ± S.E.M.

binding site. Gd^{3+} however, is not an endogenous agonist for CaSR, and many amino acids need a basal level of Ca^{2+} present to act at the CaSR. Therefore, we confirmed that ADMA also modulates Ca^{2+} stimulated CaSR activation. HEK-CaSR cells were incubated in the same HEPES buffer supplemented with 0.3 mM Ca^{2+}. Using intracellular Ca^{2+} mobilisation to visualise CaSR activation ADMA (10 μM) significantly shifted the dose-response curve leftward compared to the PBS control. This was very similar to the effect of pre-treatment with the known CaSR modulator phenylalanine (100 μM) (Fig. 5g; EC_{50} - Control 1.7 mM Ca^{2+} ± 0.19, EC_{50} - Phenylalanine 0.76 mM Ca^{2+} ± 0.11, EC_{50} - ADMA 1.1 mM Ca^{2+} ± 0.10, $P < 0.05$). In contrast neither L-arginine nor SDMA had any effect on intracellular Ca^{2+} mobilisation even in the presence of significant extracellular Ca^{2+} concentrations (Fig. 5h).

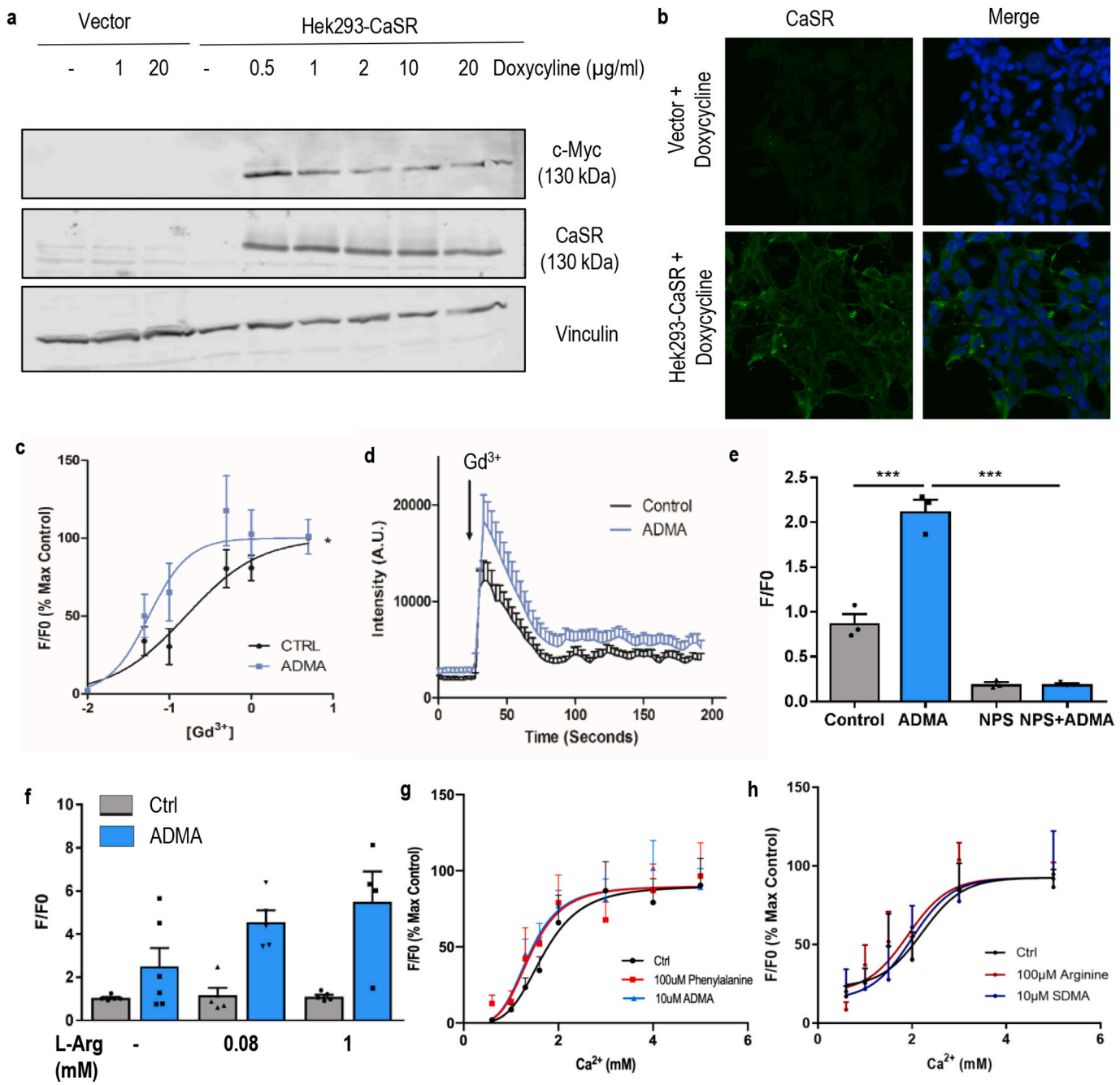

Fig. 5. ADMA is a positive allosteric modulator for CaSR. HEK293-CaSR cells were cultured with doxycycline for 24 h to stimulate CaSR expression as shown by **(a)** western blot and **(b)** immunostaining for CaSR and DAPI, data are representative images of 3 independent experiments. **(c-f)** HEK293-CaSR cells in a Ca^{2+}-free salt solution were incubated with Cal520 Ca^{2+} sensitive dye and stimulated with increasing concentrations of Gd^{3+} alone or in the presence of 10 µM ADMA. **(c)** Dose-response curve, change in intensity from baseline normalised to the 100% response in control cells (N = 12). **(d)** A representative trace of one experiment made from an average of 10 single cells analysed; 0.05 mM Gd^{3+} added at the arrow. **(e)** Cells were stimulated with 0.05 mM Gd^{3+} in the presence of 10 µM ADMA ±10 µM NPS-2143 ($N = 3$). **(f)** 0.05 mM Gd stimulation in the presence of varying arginine concentrations (N = 5). **(g and h)** HEK293-CaSR incubated with Cal520 dye were cultured in 0.3 mM Ca^{2+} before being stimulated with increasing doses of Ca^{2+} in the presence of **(g)** 100 µM Phenylalanine or 10 µM ADMA (N = 6) and **(h)** 100 µM Arginine or 10 µM SDMA. One-way ANOVA with Bonferroni *post-hoc* test was used in **e** and **f**; non-linear regression in **c**, **g and h.** * $P < 0.05$, ** $P < 0.01$, *** $P < 0.001$. Data are presented as mean ± S.E.M.

3.6. SDMA may compete with ADMA at the amino acid site on CaSR

As a range of amino acid species are known to bind CaSR and modulate its signalling, it is interesting that ADMA causes adipocyte hypertrophy whereas the methylarginine analogue SDMA does not (Fig. 1a and b). Therefore, we modelled both ADMA and SDMA within the CaSR amino acid binding site to determine whether their interaction with CaSR may provide a possible explanation. L-Tryptophan has previously been shown to bind CaSR [31]; the superimposition of ADMA within this site (Fig. 6a) shows both the amino acid moiety and guanidine are well accommodated. The alkyl sidechain makes close interactions with hydrophobic residues on the opposite side of the "hinge" region, particularly Ile416. The overlay of SDMA with ADMA (Fig. 6b) shows that again the amino acid and guanidine are accommodated, however, the differing methylation state of SDMA impacts how the alkyl portion of the side chain can be accommodated. The close interactions

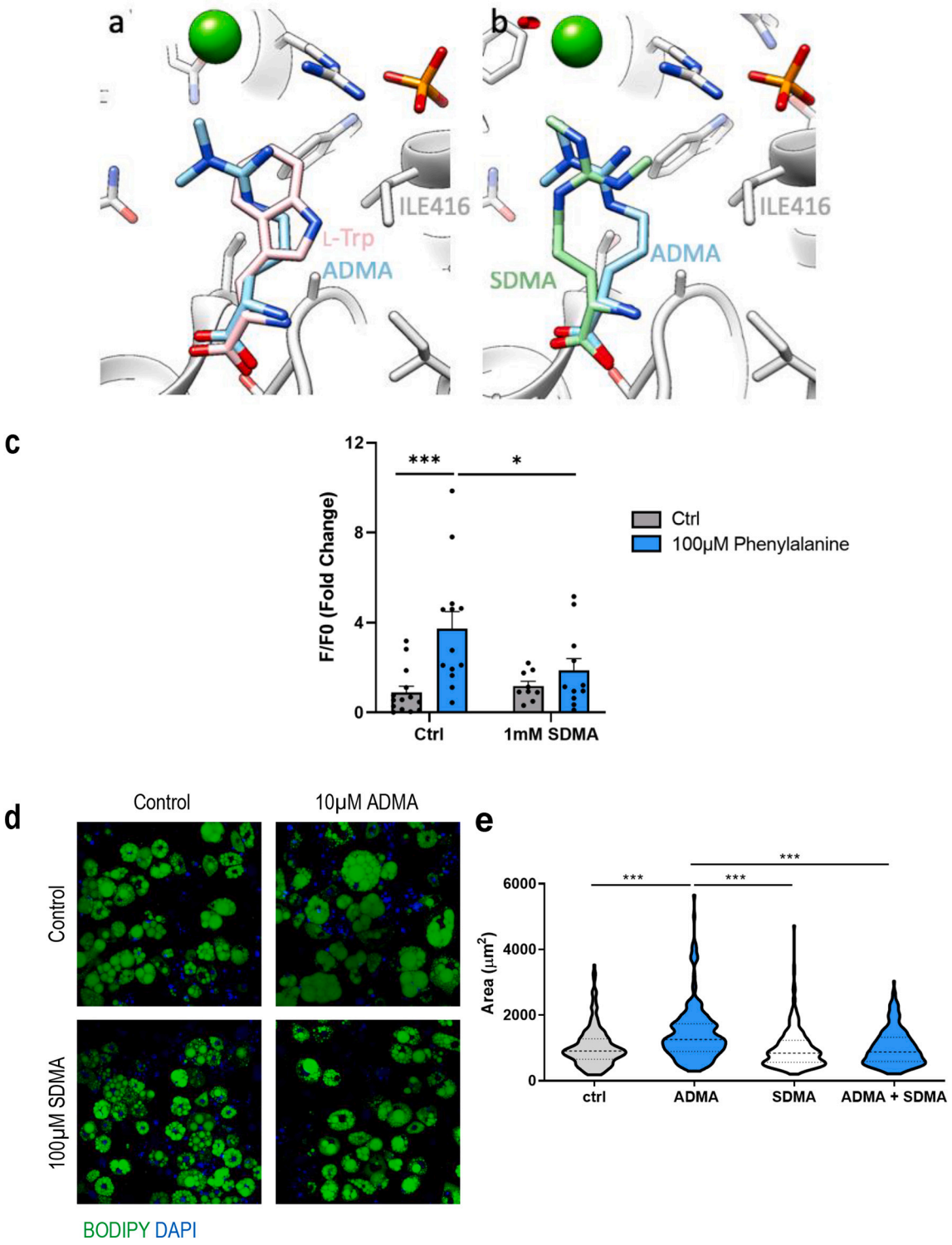

Fig. 6. SDMA can act as a competitive inhibitor of ADMA. The active form of CaSR was modelled in Autodock Vina to predict the binding of ADMA in the L-Trp binding pocket **(a)** and to compare the binding of SDMA with ADMA **(b)**. **(c)** HEK293-CaSR cells were incubated with Cal520 Ca^{2+} sensitive dye and stimulated with 1.6 mM Ca^{2+} in the presence of 100 μM phenylalanine with or without 1 mM SDMA ($N = 14$). 3T3-L1 cells were incubated for 72 h with 10 μM ADMA in the presence of 100 μM SDMA **(d)** stained with BODIPY and DAPI, (data are representative images from 4 independent experiments), and **(e)** measured for cell size. (From 4 independent experiments). One-way ANOVA with Bonferroni *post-hoc* tests was used in **c** and **e.** $^*P < 0.05$.

observed between ADMA and Ile416 are not replicated by docked SDMA due to the alternative positioning required to accommodate the symmetrical N^{ω}-methylation. These results provide supporting evidence for L-ADMA binding at the L-Trp site and are consistent with our finding that ADMA can serve as an positive allosteric modulator for CaSR by making interactions that reinforce the closed conformation of CaSR, and that SDMA does not. Given that SDMA seems to be able to bind to CaSR but perhaps not actively modulate it we hypothesised that SDMA may act to antagonise positive allosteric binding. Incubation of HEK-CaSR cells with 100 μM phenylalanine increased intracellular Ca^{2+}

mobilisation in response to stimulation with 1.6 mM Ca^{2+} (Fig. 6c) as previously demonstrated in Fig. 5h. Co-incubation with 1 mM SDMA significantly suppressed the effect of phenylalanine suggesting competition at the binding site. Finally, to determine whether SDMA has a physiological effect on CaSR activity we incubated differentiated 3T3-L1 cells with 10 μM ADMA in the absence or presence of excess (100 μM) SDMA (Fig. 6d and e). The presence of SDMA blocked ADMA driven adipocyte hypertrophy suggesting that the ADMA/SDMA ratio may be an important modulator of ADMA-CaSR signalling.

4. Discussion

ADMA is an independent risk factor for cardiovascular disease with elevated plasma concentrations associated with obesity in clinical studies [8,9,12,13]. However, an increase in the plasma concentration of many amino acids has been observed in obesity [32]; therefore, we set out to establish whether ADMA is simply a marker of metabolic disease or a mediator of disease pathology and progression. Here we show for the first time that ADMA has a direct effect on adipocyte physiology and propose a new mechanism through which excess ADMA leads to lipid accumulation via modulation of the calcium-sensing receptor (CaSR).

To examine what role ADMA plays in adipocyte physiology we employed the well characterised 3T3-L1 model, in which we established that prolonged (72 h) exposure to ADMA increased cellular lipid content. In keeping with this, ADMA upregulated the mTOR-SREBP1 pathway leading to increased transcription of the lipogenesis genes FASN, ACC and HMGCR. Similarly, liver derived HepG2 cells demonstrated lipid accumulation when treated with ADMA suggesting this pathway is not exclusively restricted to adipocytes and may be a common feature among lipogenic cells. Interestingly, mice harbouring the global deletion of the key gene involved in ADMA metabolism, dimethylarginine dimethylaminohydrolase 1 (DDAH1), gain more weight that wildtypes when placed on a high fat diet with an associated increase in lipid accumulation within the liver suggesting this pathway may also occur in vivo [33].

ADMA is a competitive inhibitor of all three NOS isoforms [2,4]. However, unexpectedly the synthetic NOS inhibitors L-NAME and PBITU did not replicate ADMA driven adipocyte hypertrophy or upregulation of mTOR expression in cell culture models. Our data indicates that ADMA has significant NO-independent biological effects at pathophysiological concentrations (1–3 μM). Cardounel et al. [34] have calculated that these low concentrations would lead to at most a 10% inhibition of NOS. In contrast, plasma concentrations of ADMA that are capable of producing significant NOS blockade are only reached during the later stages of chronic kidney disease [2]. Taken together these observations suggest that a concentration dependent shift in the balance of ADMA signalling from NO-independent mechanisms towards direct NOS inhibition may play a significant role in the loss of cellular homeostasis that underlies human disease. Consistent with this hypothesis, elevation of plasma ADMA concentrations by on average 0.3 μM from ~0.58 μM to ~0.86 μM have been observed in metabolic disorders whereas increases of 1.0–2.0 μM are found in cardiovascular disease states associated with chronic renal failure.

Previous studies have suggested that ADMA may have actions in addition to NOS inhibition. Our group examined the effect of physiological and pathophysiological concentrations of ADMA on cultured endothelial cells. We identified ~50 genes that were regulated in response to ADMA and demonstrated that for some of these genes the effect was not replicated by a synthetic NOS inhibitor (L-NIO) [35]. The pathways regulated by ADMA included BMP and Osteocalcin signalling both of which have been shown to be regulated by CaSR. Our identification of a novel ADMA/CaSR signalling pathway now provides a plausible mechanism that might mediate these effects. Further studies will be required to elucidate the full range of ADMA/CaSR signalling in different cells and tissues. In addition to our own observations, Juretic and co-workers [36] have reported that the induction of IL-2 by L-NMMA treatment in cultured peripheral blood mononucleated cells (PBMCs) was not replicated by synthetic inhibitors of NOS. Further work will be needed to establish whether L-NMMA can interact with and modulation CaSR activity.

Our data for the first time identifies a NO-independent receptor for ADMA, the amino acid sensitive GPCR CaSR. CaSR has been previously implicated in lipid homeostasis and its expression has been shown to be upregulated in fully differentiated adipocytes [37], although this was not an effect we saw in our study. The CaSR agonist $GdCl_3$ increases lipid accumulation and pro-adipogenic gene expression in the SW872 preadipocyte cell line [37]; while cinacalcet increases HepG2 triglyceride content in culture [26]. Furthermore, Rybchyn et al. [38] have recently demonstrated CaSR-mediated activation of mTOR complex 2 signalling leading to increased phosphorylation of AKT. Interestingly, this study highlights the importance of the scaffolding protein homer-1 as a key player in linking CaSR to mTOR signalling. Currently, our hypothesis, built on our modelling studies, is that ADMA binds directly to the amino acid site of CaSR and alter its activity. However, further work including binding studies and mutations of the possible binding site will be necessary to fully understand whether ADMA can bind CaSR directly or alter CaSR activity by modifying CaSR protein complexes.

Whilst ADMA competes with L-arginine for binding to the active site of NOS our data indicates that arginine is unable to compete with ADMA for CaSR. The literature relating to L-arginine binding to CaSR is somewhat contradictory with some studies reporting no effect of basic amino acids on the receptor [30] while others report a strong stimulation of CaSR by L-arginine in the gut [39]. In our hands, L-arginine had no effect on the expression lipogenic genes in either 3T3-L1 or HepG2 cells. Furthermore, using stably transfected HEK293 cells, L-arginine was unable to directly activate CaSR or modulate the effect of ADMA on the receptor. L-arginine activation of CaSR in particular, seems sensitive to the prevailing Ca^{2+} concentration only showing a low potency to activate CaSR at around 2 mM Ca^{2+} and therefore, the relatively modest calcium concentrations in DMEM (1.8 mM) may mask the full effect of L-arginine on CaSR activity [40]. ADMA increased CaSR sensitivity to Gd^{3+} and Ca^{2+} in its physiological range (low μM) suggests greater affinity for CaSR than the known CaSR modulators *L*-phenylalanine and L-tryptophan both of which have been shown to act in the mM range [31]. SDMA alone equally had no effect on lipogenesis or CaSR activity, however, we show initial studies which suggest SDMA is able to block the effect of ADMA and phenylalanine on CaSR. These observations are of potential physiological importance as elevated SDMA concentrations are also considered an independent factor for cardiovascular risk [41] but, to date, no mechanism of action that can explain this association has been identified. Our in silico modelling studies suggest that both ADMA and SDMA can bind in the amino acid binding pocket of CaSR that crystallographic studies have demonstrated is occupied by tryptophan. Both methylated arginine molecules are predicted to bind with equal affinity however only ADMA is predicted to interact with Ile416 in the activation loop of CaSR. These observations provide a potential molecular explanation of the effects of ADMA/SDMA on CaSR activity. Structural studies with mutations within the potential binding site will be required to fully understand the structure/activity relationships of ADMA/SDMA:CaSR and the impact of genetic variants in CaSR on methylarginine signalling via this receptor.

Our identification of an ADMA-CaSR signalling pathway that is sensitive to small changes in ADMA concentration in the micromolar range and is independent of prevailing arginine concentrations, provides a potential mechanistic explanation of the association between ADMA and cardiovascular and metabolic risk, therefore offering novel therapeutic opportunities to mitigate the effects of elevated ADMA. Further studies will be required to fully understand the significance of ADMA signalling via GPCRs particularly in the cardiovascular system.

Author contributions

Conceptualization : J.L, L.Dowsett. Investigation: L.Dowsett, L. Duluc, E.H., F.A, I.S. and W.F. Formal Analysis: L.Dowsett, L.Duluc. Funding Acqusition: J.L. Supervision: J.L and I.S. Writing - original draft: L. Dowsett and L. Duluc. Writing - reviewing and editing: E.H, I.S, J,.L. Correspondence and request for material should be addressed to J.L (james.leiper@glasgow.ac.ukmailto:) or to L.Dowsett (laura.dowsett@glasgow.ac.uk).

Declaration of Competing Interest

JL is a founder, director and shareholder of Critical Pressure Ltd., Cambridge, UK.

Data availability

Data will be made available on request.

Acknowledgements

We would like to thank Prof. Graeme Milligan for the gift of the Flp-In T-REX cell line. This study was supported by MRC intramural funding to J.L and British Heart Foundation Centre of Research Excellence Award (RE/13/5/30177).

Appendix A. Supplementary data

Supplementary data to this article can be found online at https://doi.org/10.1016/j.cellsig.2023.110676.

References

[1] M.T. Bedford, S.G. Clarke, Protein arginine methylation in mammals: who, what, and why, Mol. Cell 33 (1) (2009) 1–13.
[2] P. Vallance, A. Leone, A. Calver, J. Collier, S. Moncada, Accumulation of an endogenous inhibitor of nitric oxide synthesis in chronic renal failure, Lancet 339 (8793) (1992) 572–575.
[3] P. Vallance, A. Leone, A. Calver, J. Collier, S. Moncada, Endogenous dimethylarginine as an inhibitor of nitric oxide synthesis, J. Cardiovasc. Pharmacol. 20 (Suppl. 12) (1992) S60–S62.
[4] A.J. Cardounel, J.L. Zweier, Endogenous methylarginines regulate neuronal nitric-oxide synthase and prevent excitotoxic injury, J. Biol. Chem. 277 (37) (2002) 33995–34002.
[5] J. Leiper, M. Nandi, B. Torondel, J. Murray-Rust, M. Malaki, B. O'Hara, S. Rossiter, S. Anthony, M. Madhani, D. Selwood, C. Smith, B. Wojciak-Stothard, A. Rudiger, R. Stidwill, N.Q. McDonald, P. Vallance, Disruption of methylarginine metabolism impairs vascular homeostasis, Nat. Med. 13 (2) (2007) 198–203.
[6] R.H. Boger, S.M. Bode-Boger, A. Szuba, P.S. Tsao, J.R. Chan, O. Tangphao, T. F. Blaschke, J.P. Cooke, Asymmetric dimethylarginine (ADMA): a novel risk factor for endothelial dysfunction: its role in hypercholesterolemia, Circulation 98 (18) (1998) 1842–1847.
[7] S. Lambden, P. Kelly, B. Ahmetaj-Shala, Z. Wang, B. Lee, M. Nandi, B. Torondel, M. Delahaye, L. Dowsett, S. Piper, J. Tomlinson, B. Caplin, L. Colman, O. Boruc, A. Slaviero, L. Zhao, E. Oliver, S. Khadayate, M. Singer, F. Arrigoni, J. Leiper, Dimethylarginine dimethylaminohydrolase 2 regulates nitric oxide synthesis and hemodynamics and determines outcome in polymicrobial sepsis, Arterioscler. Thromb. Vasc. Biol. 35 (6) (2015) 1382–1392.
[8] H.M. Eid, H. Arnesen, E.M. Hjerkinn, T. Lyberg, I. Seljeflot, Relationship between obesity, smoking, and the endogenous nitric oxide synthase inhibitor, asymmetric dimethylarginine, Metabolism 53 (12) (2004) 1574–1579.
[9] H. Kocak, Y. Oner-Iyidogan, F. Gurdol, P. Oner, D. Esin, Serum asymmetric dimethylarginine and nitric oxide levels in obese postmenopausal women, J. Clin. Lab. Anal. 25 (3) (2011) 174–178.
[10] T. McLaughlin, M. Stuhlinger, C. Lamendola, F. Abbasi, J. Bialek, G.M. Reaven, P. S. Tsao, Plasma asymmetric dimethylarginine concentrations are elevated in obese insulin-resistant women and fall with weight loss, J. Clin. Endocrinol. Metab. 91 (5) (2006) 1896–1900.
[11] I. Palomo, A. Contreras, L.M. Alarcon, E. Leiva, L. Guzman, V. Mujica, G. Icaza, N. Diaz, D.R. Gonzalez, R. Moore-Carrasco, Elevated concentration of asymmetric dimethylarginine (ADMA) in individuals with metabolic syndrome, Nitric Oxide 24 (4) (2011) 224–228.
[12] M. El Assar, J. Angulo, M. Santos-Ruiz, J.C. Ruiz De Adana, M.L. Pindado, A. Sánchez-Ferrer, A. Hernández, L. Rodríguez-Mañas, Asymmetric dimethylarginine (ADMA) elevation and arginase up-regulation contribute to endothelial dysfunction related to insulin resistance in rats and morbidly obese humans, J. Physiol. 594 (11) (2016) 3045–3060.
[13] Y. Arlouskaya, A. Sawicka, M. Głowala, J. Giebułtowicz, N. Korytowska, M. Tałałaj, G. Nowicka, M. Wrzosek, Asymmetric Dimethylarginine (ADMA) and symmetric Dimethylarginine (SDMA) concentrations in patients with obesity and the risk of obstructive sleep apnea (OSA), J. Clin. Med. 8 (6) (2019) 897.
[14] W. Lee, H.J. Lee, H.B. Jang, H.-J. Kim, H.-J. Ban, K.Y. Kim, M.S. Nam, J.S. Choi, K.-T. Lee, S.B. Cho, S.I. Park, H.-J. Lee, Asymmetric dimethylarginine (ADMA) is identified as a potential biomarker of insulin resistance in skeletal muscle, Sci. Rep. 8 (1) (2018).
[15] M. El Assar, J. Angulo, M. Santos-Ruiz, J.C. Ruiz de Adana, M.L. Pindado, A. Sanchez-Ferrer, A. Hernandez, L. Rodriguez-Manas, Asymmetric dimethylarginine (ADMA) elevation and arginase up-regulation contribute to endothelial dysfunction related to insulin resistance in rats and morbidly obese humans, J. Physiol. 594 (11) (2016) 3045–3060.
[16] K. Krzyzanowska, F. Mittermayer, H.P. Kopp, M. Wolzt, G. Schernthaner, Weight loss reduces circulating asymmetrical dimethylarginine concentrations in morbidly obese women, J. Clin. Endocrinol. Metab. 89 (12) (2004) 6277–6281.
[17] J.W. Choi, S.H. Pai, S.K. Kim, M. Ito, C.S. Park, Y.N. Cha, Increases in nitric oxide concentrations correlate strongly with body fat in obese humans, Clin. Chem. 47 (6) (2001) 1106–1109.
[18] M. Elizalde, M. Ryden, V. van Harmelen, P. Eneroth, H. Gyllenhammar, C. Holm, S. Ramel, A. Olund, P. Arner, K. Andersson, Expression of nitric oxide synthases in subcutaneous adipose tissue of nonobese and obese humans, J. Lipid Res. 41 (8) (2000) 1244–1251.
[19] R.J. Ward, E. Alvarez-Curto, G. Milligan, Using the Flp-in T-rex system to regulate GPCR expression, Methods Mol. Biol. 746 (2011) 21–37.
[20] J.G. Boyle, P.J. Logan, G.C. Jones, M. Small, N. Sattar, J.M. Connell, S.J. Cleland, I. P. Salt, AMP-activated protein kinase is activated in adipose tissue of individuals with type 2 diabetes treated with metformin: a randomised glycaemia-controlled crossover study, Diabetologia 54 (7) (2011) 1799–1809.
[21] T. Porstmann, C.R. Santos, C. Lewis, B. Griffiths, A. Schulze, A new player in the orchestra of cell growth: SREBP activity is regulated by mTORC1 and contributes to the regulation of cell and organ size, Biochem. Soc. Trans. 37 (Pt 1) (2009) 278–283.
[22] S. Elms, F. Chen, Y. Wang, J. Qian, B. Askari, Y. Yu, D. Pandey, J. Iddings, R. B. Caldwell, D.J. Fulton, Insights into the arginine paradox: evidence against the importance of subcellular location of arginase and eNOS, Am. J. Physiol. Heart Circ. Physiol. 305 (5) (2013) H651–H666.
[23] J. Strobel, M. Mieth, B. Endress, D. Auge, J. Konig, M.F. Fromm, R. Maas, Interaction of the cardiovascular risk marker asymmetric dimethylarginine (ADMA) with the human cationic amino acid transporter 1 (CAT1), J. Mol. Cell. Cardiol. 53 (3) (2012) 392–400.
[24] M. Cifuentes, C. Fuentes, P. Mattar, N. Tobar, E. Hugo, N. Ben-Jonathan, C. Rojas, J. Martinez, Obesity-associated proinflammatory cytokines increase calcium sensing receptor (CaSR) protein expression in primary human adipocytes and LS14 human adipose cell line, Arch. Biochem. Biophys. 500 (2) (2010) 151–156.
[25] R. Bravo-Sagua, P. Mattar, X. Diaz, S. Lavandero, M. Cifuentes, Calcium sensing receptor as a novel mediator of adipose tissue dysfunction: mechanisms and potential clinical implications, Front. Physiol. 7 (2016) 395.
[26] P. Villarroel, P. Mattar, A. D'Espessailles, M. Arrese, A. Arreguin, C. Fuentes, M. Reyes, M. Cifuentes, Calcium sensing receptor effects in adipocytes and liver cells: implications for an adipose-hepatic crosstalk, Arch. Biochem. Biophys. 607 (2016) 47–54.
[27] A.D. Conigrave, D.R. Hampson, Broad-spectrum amino acid-sensing class C G-protein coupled receptors: molecular mechanisms, physiological significance and options for drug development, Pharmacol. Ther. 127 (3) (2010) 252–260.
[28] L. Chun, W.H. Zhang, J.F. Liu, Structure and ligand recognition of class C GPCRs, Acta Pharmacol. Sin. 33 (3) (2012) 312–323.
[29] Y.H. He, Y. He, X.L. Liao, Y.C. Niu, G. Wang, C. Zhao, L. Wang, M.J. Tian, Y. Li, C. H. Sun, The calcium-sensing receptor promotes adipocyte differentiation and adipogenesis through PPARgamma pathway, Mol. Cell. Biochem. 361 (1–2) (2012) 321–328.
[30] A.D. Conigrave, D.T. Ward, Calcium-sensing receptor (CaSR): pharmacological properties and signaling pathways, Best Pract. Res. Clin. Endocrinol. Metab. 27 (3) (2013) 315–331.
[31] C. Zhang, T. Zhang, J. Zou, C.L. Miller, R. Gorkhali, J.Y. Yang, A. Schilmiller, S. Wang, K. Huang, E.M. Brown, K.W. Moremen, J. Hu, J.J. Yang, Structural basis for regulation of human calcium-sensing receptor by magnesium ions and an unexpected tryptophan derivative co-agonist, Sci. Adv. 2 (5) (2016), e1600241.
[32] C.S. Katsanos, L.J. Mandarino, Protein metabolism in human obesity: a shift in focus from whole-body to skeletal muscle, Obesity (Silver Spring) 19 (3) (2011) 469–475.
[33] T. Li, R. Feng, C. Zhao, Y. Wang, J. Wang, S. Liu, J. Cao, H. Wang, T. Wang, Y. Guo, Z. Lu, Dimethylarginine Dimethylaminohydrolase 1 protects against high-fat diet-induced hepatic steatosis and insulin resistance in mice, Antioxid. Redox Signal. 26 (11) (2017) 598–609.
[34] A.J. Cardounel, H. Cui, A. Samouilov, W. Johnson, P. Kearns, A.L. Tsai, V. Berka, J. L. Zweier, Evidence for the pathophysiological role of endogenous methylarginines in regulation of endothelial NO production and vascular function, J. Biol. Chem. 282 (2) (2007) 879–887.
[35] C.L. Smith, S. Anthony, M. Hubank, J.M. Leiper, P. Vallance, Effects of ADMA upon gene expression: an insight into the pathophysiological significance of raised plasma ADMA, PLoS Med. 2 (10) (2005), e264.
[36] A. Juretic, G.C. Spagnoli, H. Horig, T. Gross, H. Gallati, M. Samija, D. Eljuga, M. Turic, F. Harder, M. Heberer, Nitric oxide-independent inhibitory effects of L-

arginine analog NG-monomethy-L-arginine on the generation of interleukin-2 activated cytotoxic activity in humans, Clin. Nutr. 15 (1) (1996) 16–20.
[37] Y. He, H. Zhang, J. Teng, L. Huang, Y. Li, C. Sun, Involvement of calcium-sensing receptor in inhibition of lipolysis through intracellular cAMP and calcium pathways in human adipocytes, Biochem. Biophys. Res. Commun. 404 (1) (2011) 393–399.
[38] M.S. Rybchyn, K.S. Islam, T.C. Brennan-Speranza, Z. Cheng, S.C. Brennan, W. Chang, R.S. Mason, A.D. Conigrave, Homer1 mediates CaSR-dependent activation of mTOR complex 2 and initiates a novel pathway for AKT-dependent beta-catenin stabilization in osteoblasts, J. Biol. Chem. 294 (44) (2019) 16337–16350.
[39] O.J. Mace, M. Schindler, S. Patel, The regulation of K- and L-cell activity by GLUT2 and the calcium-sensing receptor CasR in rat small intestine, J. Physiol. 590 (12) (2012) 2917–2936.
[40] A.D. Conigrave, H.C. Mun, L. Delbridge, S.J. Quinn, M. Wilkinson, E.M. Brown, L-amino acids regulate parathyroid hormone secretion, J. Biol. Chem. 279 (37) (2004) 38151–38159.
[41] S. Schlesinger, S.R. Sonntag, W. Lieb, R. Maas, Asymmetric and symmetric Dimethylarginine as risk markers for Total mortality and cardiovascular outcomes: a systematic review and Meta-analysis of prospective studies, PLoS One 11 (11) (2016), e0165811.